DETERMINATION OF ENERGY GAP OF THE IRON-BASED OXYPNICTIDE AND LaOFeGe SUPERCONDUCTORS USING SPECIFIC HEAT CAPACITY

TAREK MOHAMED FAYEZ AHMAD

UNIVERSITI SAINS MALAYSIA

2013

DETERMINATION OF ENERGY GAP OF THE IRON-BASED OXYPNICTIDE AND LaOFeGe SUPERCONDUCTORS USING SPECIFIC HEAT CAPACITY

By

TAREK MOHAMED FAYEZ AHMAD

Thesis submitted in fulfillment of the requirements
for the degree of
Doctor of Philosophy

October 2013

DEDICATION

To my father and mother

To my brothers and sisters

To my wife and my sons

ACKNOWLEDGMENTS

First and foremost, I give praise and thanks to the almighty Allah for giving me the strength to complete my research study.

I would like to express my sincerest and deepest gratitude to my fatherly supervisor Professor Kamarulazizi Bin Ibrahim for his wisdom, guidance, and intellectual support. His encouraging attitude and self-less guidance throughout the years have enriched me with empirical insights and knowledge in my scientific and academic career.

I would like to thank Universiti Sains Malaysia for their generous financial support. I also thank the staff members of the School of Physics for the co-operation, technical assistance, and support they extended during my studies.

Finally, I thank my friends for encouraging and helping me throughout my journey in the academe.

Tarek Mohamed Fayez Ahmad

Penang, Malaysia. 2013

LIST OF TABLES

LIST OF FIGURES

LIST OF SYMBOLS

a	a-axis lattice constant
c	c-axis lattice constant
C	Specific heat
$C_{n,e}$	Normal electronic specific heat
$C_{s,e}$	Superconducting electronic specific heat
$C_{n,ph}$	Normal phonon specific heat
$C_{s,ph}$	Superconducting phonon specific heat
d	Distance between volt-ammeter electrodes
E_F	Fermi level
(hkl)	Miller indices
I	Current
J	Hund's-rule interaction
k_B	Boltzmann constant
k	Geometric factor
n_s	Density of super electrons
n_n	Density of normal electrons
n	Density of conduction electrons
R	Resistance
S	Cross section of the sample
T	Temperature
t	Time
T_{anom}	Anomaly transition point of resistivity $\rho(T)$
T_c	Critical transition temperature
T_{mag}	Magnetic transition temperature
$T_{midpoint}$	Midpoint transition temperature of resistivity $\rho(T)$
T_N	Neel temperature
$T_{\rho\approx0}$	zero resistivity transition temperature
T_{onset}	Onset transition temperature of resistivity $\rho(T)$
T_s	Structural transition temperature
T_{Sm}	Samarium ordering temperature
U	Hubbard interaction
V	Voltage
z_{Ln}	Ln–O interlayer spacings (Ln=rare-reath)
z_{Pn}	M–Pn interlayer spacings (M=transition metals, Pn=pnictogen)
θ	Incident / Diffraction angle
Θ_D	Debye temperature
ρ	Resistivity
ρ_0	Residual resistivity
ω	Photon frequency
λ	Wavelength
Δ	Energy gap
α	As–Fe–As bond angle
β	AsAs–Fe–As bond angle
β_1	Lattice heat capacity coefficient
γ	Electronic heat capacity coefficient
γ_n	Normal electronic heat capacity coefficient
γ_{sc}	Superconducting electronic heat capacity coefficient

LIST OF MAJOR ABBREVIATIONS

a.u.	Arbitrary unit
AFM	Antiferromagnetic
ARPES	Angle-resolved photoemission spectroscopy
BCS	Bardeen-Cooper-Schrieffer theory
DFT	Density functional theory
eV	Electron volt
FTIR	Fourier transform infrared
GT	Gutzwiller variational theory
PCS	Point-contact spectroscopy
PES	Photoemission spectroscopy
PM	Paramagnetic
ρ-T	Resistivity-temperature
SDW	Spin density wave
XRD	X-ray diffraction

PENENTUAN JURANG TENAGA DARIPADA OKSIPIKTIDA BERASASKAN FERUM DAN SUPERKONDUKTOR LaOFeGe MENGGUNAKAN KAPASITI HABA TENTU

ABSTRAK

Indikator atau petunjuk kesuperkonduksian yang paling utama adalah suhu peralihan (T_c) dan jurang tenaga kesuperkonduksian (Δ). Petunjuk ini dikaitkan dengan keadaan suhu elektronik yang bergantung pada ukuran kerintangan dan haba pendam, masing-masing. Haba tentu ini adalah suatu ukuran pukal yang memantulkan atau menggambarkan perlakuan keseluruhan respons sampel. Dalam penyelidikan ini, kami memperkenalkan suatu model bagi mengkaji ciri-ciri peralihan keadaan superkonduksian normal pada suhu kritikal daripada sumbangan elektron dan fonon haba tentu. Tiga postulat asas disesuaikan. Pertama, peralihan sistem daripada keadaan normal kepada keadaan superkonduksian, yang membolehkan fonon mengikat electron untuk membentuk pasangan Cooper, yang memerlukan perubahan dalam tenaga yang berbeza, yang wujud dalam perlakuan haba tentu. Kedua, haba tentu mempunyai sumbangan yang berbeza, yang boleh berubah secara berbeza pada T_c. Perubahan ini mungkin terhasil daripada fungsi fizikal terhadap sumbangan tersebut. Ketiga, perlakuan fonon yang boleh menjelaskan sifat superkonduksian, terutamanya dalam keadaan sedia ada.

Berasaskan model peralihan superkonduksian yang dicadangkan, yang dibina bergantung pada perlakuan superkonduksian haba tentu yang selaras dengan postulat di atas, maka diperoleh skala tenaga pada keadaan normal bagi oksipiktida berasaskan ferum. Keadaan pseudojurang normal 2Δ adalah 14.26 meV bagi sebatian $SmO_{0.80}F_{0.20}FeAs$, yang ditentukan daripada spectrum pantulan inframerah jauh berdasarkan keadaan fonon pada suhu bilik. Jurang tenaga superkonduksian 2Δ

adalah 7.61 meV bagi $LaO_{0.9}F_{0.1}FeAs$, yang dikira daripada haba tentu fonon normal. Selanjutnya, model peralihan superkonduksian diaplikasikan pada data eksperimen haba tentu sebatian $LnO_{1-x}F_xFeAs$ (Ln=La, Sm). Takat peralihan daripada keadaan normal kepada keadaan superkonduksian bagi model ini adalah pada titik tengah suhu peralihan, yang diperoleh daripada ukuran kerintangan, dengan 22.11 K dan 26.32 K daripada $LaO_{0.9}F_{0.1}FeAs$ dan $SmO_{0.87}F_{0.13}FeAs$, masing-masing

Sebatian $LaO_{1-x}F_xFeGe$ berasaskan ferum, dengan Ge dalam lapisan konduksi, disintesis menggunakan keadah tindak balas keadaan pepejal dua-langkah. Dalam pengukuran kerintangan elektrik $\rho(T)$, sebatian induk LaOFeGe menunjukkan anomali yang jelas (T_{anom}) pada 90 K, yang lebih kecil daripada 150 K bagi ferum-oksipiktida LnOFeAs (Ln=La, Sm, Ce, Gd). Selanjutnya, keluk kerintangan mempamerkan suatu peralihan rintangan yang diaruh oleh F-doping bagi $LaO_{1-x}F_xFeGe$, dengan suhu peralihan kerintangan *onset* (T_{onset}) adalah 19.7 K dan 21.3 K bagi sampel dengan $x = 0.11$ dan $x = 0.13$. Pengukuran pantulan inframerah jauh menunjukkan bahawa Ge adalah peka atau sensitif terhadap perubahan perlakuan fonon Perubahan ini berlaku semasa peralihan sifat fonon daripada fasa LaOFeGe kepada fasa superkonduksian $LaO_{1-x}F_xFeGe$ (x=0.11, 0.13), termasuk sifat fonon termampat. Model peralihan superkonduksian diaplikasikan bagi data eksperimen spektrum pantulan pada suhu bilik bagi $LaO_{1-x}F_xFeGe$ (x=0, 0.11, 0.13). Sebagai hasilnya, diperoleh jurang tenaga pada $2\Delta=2.097$ meV bagi $LaO_{0.89}F_{0.11}FeGe$

DETERMINATION OF ENERGY GAP OF THE IRON-BASED OXYPNICTIDE AND LaOFeGe SUPERCONDUCTORS USING SPECIFIC HEAT CAPACITY

ABSTRACT

The most prominent indicators of superconductivity are the superconducting transition temperature (T_c) and the superconducting energy gap (Δ). These indicators associated with electronic state of temperature dependence of resistivity and specific heat measurements, respectively. The specific heat is a bulk measurement that reflects the behavior of the entire sample response. Here, we introduce a model that examines the transition characteristic to a normal/superconducting state at a critical temperature of the electron and phonon contributions of specific heat. Three basic postulates were adopted. First is that the transition of the system from normal to superconducting state, which allows phonons to bind electrons to form Cooper pairs, requiring a change in energy differences appearing in a specific heat behavior. Second, specific heat has different contributions, changing differently at T_c. This change is possibly a result of the physical function on such contributions. The third postulate is that phonon behavior can manifest superconductive property, particularly in the coexisting state.

Based on the suggested superconducting transition model, which was constructed depending on the superconductive behavior of specific heat in accordance with above postulates, energy scales were obtained at normal state for iron-based oxypnictides. The pseudogap 2Δ was 14.26 meV for the $SmO_{0.80}F_{0.20}FeAs$ compound, which was determined from the far-infrared reflectance spectra based on the phonon state at room temperature. The superconducting energy gap 2Δ was 7.61 meV for the $LaO_{0.9}F_{0.1}FeAs$, which was calculated from the normal phonon specific

heat. Furthermore, the superconducting transition model was applied to the experimental data of specific heat of $LnO_{1-x}F_xFeAs$ (Ln=La, Sm) compounds. The transition point from normal to superconducting state obtained from this model was at midpoint transition temperature obtained from the resistivity measurement, with 22.11 K and 26.32 K of $LaO_{0.9}F_{0.1}FeAs$ and $SmO_{0.87}F_{0.13}FeAs$, respectively.

Iron based $LaO_{1-x}F_xFeGe$ compound, with Ge in the conduction layer, was synthesized using a two-step solid-state reaction method. In the electrical resistivity measurement $\rho(T)$, the parent compound LaOFeGe demonstrated a clear anomaly (T_{anom}) at 90 K, which is less than 150 K for the iron-oxypnictide LnOFeAs (Ln=La, Sm, Ce, Gd). Furthermore, resistivity curves exhibited a resistive transition induced by F-doping for $LaO_{1-x}F_xFeGe$, where the onset resistivity transition temperatures (T_{onset}) were 19.7 K and 21.3 K for samples with x = 0.11 and x = 0.13. Far-infrared reflectance measurement demonstrated that Ge was sensitive to changes in phonon behavior. These changes occurred during the transition of phonon features from an LaOFeGe phase to a superconducting phase $LaO_{1-x}F_xFeGe$ (x=0.11, 0.13), including the phonon-suppressed feature. The superconducting transition model was applied to the experimental data of room temperature reflectance spectra of $LaO_{1-x}F_xFeGe$ (x=0, 0.11, 0.13). The energy gap was observed at 2Δ=2.097 meV for $LaO_{0.89}F_{0.11}FeGe$.

CHAPTER 1

INTRODUCTION

1.1 Introduction to superconductivity

Superconductivity is a physical state of low-temperature physics that occurs in certain conditions, enabling the material to transition from normal state at room temperature to superconducting state at very low temperature. When the material is cooled down with decreasing temperature until reaching a transition point referred to as transition temperature or critical temperature T_c, the electrical resistivity of the material abruptly drops to zero. Superconductivity was discovered by H. K. Onnes in 1911, when mercury (Hg) was cooled to low temperature and showed zero resistance at T_c=4.15 K [1,2].

The two main characteristics that define superconductivity are zero electrical resistance and perfect diamagnetism, where a sharp drop can be observed at a certain temperature in the curves of these properties. The superconducting state cannot exist under a magnetic field greater than the critical value. Strong applied magnetic field above the critical value causes the collapse of the superconductivity and the superconductor returns to its normal state even at below T_c. Superconductors are classified into two types depending on the critical field. Type I superconductors refer to metal superconductors, such as aluminum, zinc, lead, tantalum, vanadium, and tin. Type II superconductors refer to alloys made from elements and compounds. The highest superconducting transition temperature for Type I superconductors at ambient pressure is 9.3 K of niobium [1,2].

Type I superconductors have one critical field at the onset of the normal state, where the sample turns from superconducting state to normal state, thereby causing the superconductivity to cease. Type II superconductors have two critical field

values: one at the onset of a mixed superconducting and normal states, where the sample turns from the superconducting state to a mixed state regions; and one where the sample loses its superconductivity, in which the sample turns from the mixed state to the normal state (Fig. 1.1). Type II superconductors exhibit critical magnetic fields much higher than of that type I. Superconductors exclude an applied magnetic field and do not allow it to penetrate into its core. This behavior is called Meissner effect, which has two cases. First, if the superconducting material is cooled below T_c in the absence of an external magnetic field, and then placed in a magnetic field, the field will be excluded from the material; this case is named zero field cooled. The second case is field cooled, where an external magnetic field is applied on the same superconducting material. The field will penetrate the material in the normal state ($T > T_c$), and then cooled below T_c in the presence of the magnetic field. Finally, field will be expelled from the material [3].

The most prominent indicator of superconductivity is the superconducting transition temperature (T_c) that refers to three points (Fig. 1.2). The onset transition temperature (T_{onset}) is defined as the deviation point away from the $\rho(T)$ straight line (onset of the drop in resistivity). The midpoint transition temperature ($T_{midpoint}$) is defined as the temperature, where resistivity becomes 50% of its value at T_{onset}. The zero-resistance transition temperature ($T_{\rho\approx0}$) is defined as the temperature, in which the resistance is identically zero or only immeasurably small [4,5,6,7,8].

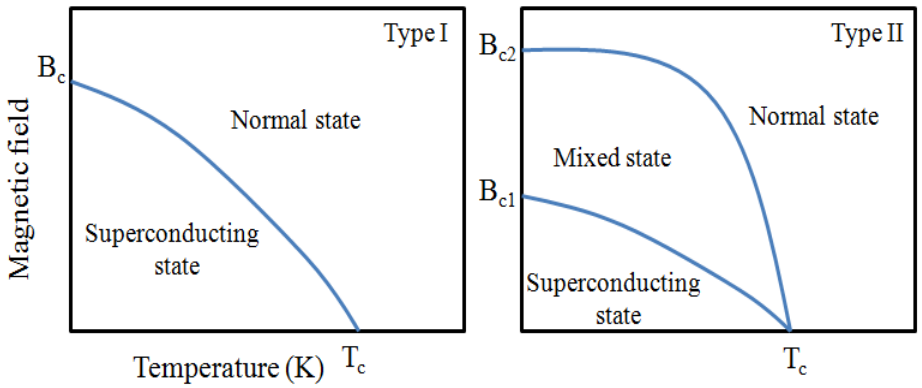

Fig. 1.1. Phase diagrams for type I and II superconductors showing magnetic field versus temperature [1].

The most important parameter of a superconductor is the superconducting energy gap created by the pairing of electrons, where all electrons with low energy pair up to certain energy range. In the paired state, two electrons are bound together at low temperatures with energy lower than the Fermi level. At $T \leq T_c$, electrons on Fermi surface form electron pairs. A gap is then opened on the Fermi surface, indicating that the Fermi surface is gapped in the superconducting state ($T=T_c$) [9,10,11,12,13]. Probing the energy gap is essential for explaining the mechanism of superconductivity, where pairing causes a gap opening in the continuous spectrum. Optical measurements can provide important information about the nature of the phase transition, where the infrared spectra from the Fourier transform infrared spectroscopy (FTIR) provides evidence for the formation of the energy gap on the Fermi surface [14,15,16,17].

The presence of the energy gap is one of the hallmarks of the theories that explain superconductivity; however, the discovery of the gap is based on the experiments on specific heat measurements for a wide range of temperature above and below the transition temperature. A jump at the transition temperature in

temperature dependence of the specific heat *C(T)* curves (Fig. 1.2) indicates the existence of a gap in the energy. Given the energy gap, the specific heat of the superconductor varies after reaching the transition temperature and is suppressed strongly at low temperatures, indicating that specific heat as well as the superconducting energy gap and T_c are all related [1,18,19,20,21,22].

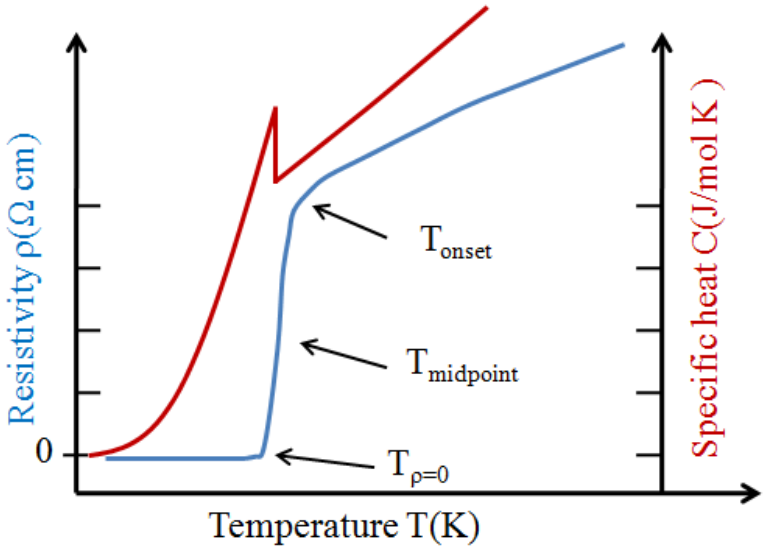

Fig.1.2. Resistivity versus temperature of a superconductor with different definitions of transition temperature. Specific heat jump is observed at T_c in the temperature dependence of specific heat [2].

The discovery of superconductivity has initiated a path of experimental work that led to the discoveries of several classes of novel superconductors; binary compounds, such as Nb_3Sn [23], Nb_3Ga [24], Nb_3Ge [25], and ZrN [26]; ternary compounds, such as Pb–Bi–Sn [27], $LaNiGa_2$ [28], AFe_2As_2 (A=Ca, Sr, Ba, Eu), and LiFeAs [29]; and quaternary compounds, such as Cuprates [30] and oxypnictides [31]. A number of superconductor classes have also been developed, including Cuprate family, which is classified as a high temperature superconductor. High T_c superconductor Cuprates are chemical compounds containing copper oxide, which

have been discovered in 1986 by Müller and Bednorz [32], where their system Ba−La−Cu−O showed T_c at 30 K. This discovery was followed by the definition of this system as RE−Ba−Cu−O superconductors, where RE is a rare earth element or yttrium. The highest transition temperature has been observed in pentanary copper oxide superconductor $Hg_{0.2}Tl_{0.8}Ba_2Ca_2Cu_3O_{8.33}$ with T_c=138 K. With external pressure, the superconducting transition goes up to 164 K in $HgBa_2Ca_2Cu_3O_{12y}$ under 30 GPa [2,30,33,34].

In 1995, Zimmer et al. [35] prepared quaternary phases of LnOMP compounds (Ln-rare-earth, M=Fe, Ru, Co), while in 2000, P. Quebe et al. [36] prepared the same compound by replacing P with As; LnOMAs. The crystal structure data of this family showed that these compounds crystallize to form a tetragonal with ZrCuSiAs type structure.

The superconducting properties of the LnOMP family have been studied by many researchers from 2006 until now. In the field of superconductivity, this family is named oxypnictides 1111-structure, LnOMPn compounds, where Ln=rare-earth, M=transition metals, and Pn=pnictogen. The study of iron-based oxypnictides has paramount importance because they contain iron, the most common ferromagnetic metal that exhibits superconductivity. The coexistence of magnetism and superconductivity in oxypnictide materials remains a subject of discussion. In $CeO_{1-x}F_xFeAs$ [37], the magnetic and superconducting phenomena do not coexist as shown in the temperature versus F-doping concentration phase diagram in Figure 1.3, where the antiferromagnetic order is suppressed before the appearance of superconductivity. A similar magnetic and superconducting phase diagram has been reported on $SmO_{1-x}F_xFeAs$ [38] (Figure 1.4) where it was revealed that static magnetism coexists with superconducting state in the range of $0.10 \leq x \leq 0.15$.

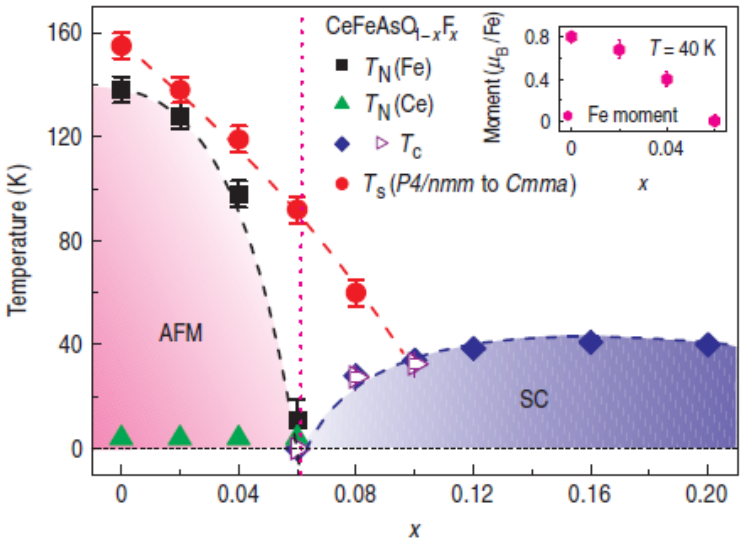

Fig. 1.3. The structural and magnetic phase diagram of $CeO_{1-x}F_xFeAs$ (x = 0, 0.02, 0.04, 0.06, 0.16). The antiferromagnetic order (AFM) vanishes before the emergence of superconductivity (SC) for x > 0.06. The red circles indicate the onset temperature of *P4/nmm* to *Cmma* phase transition. The black squares and green triangles designate the Neel temperatures of Fe (T_N(Fe)) and Ce (T_N(Ce)), respectively [37].

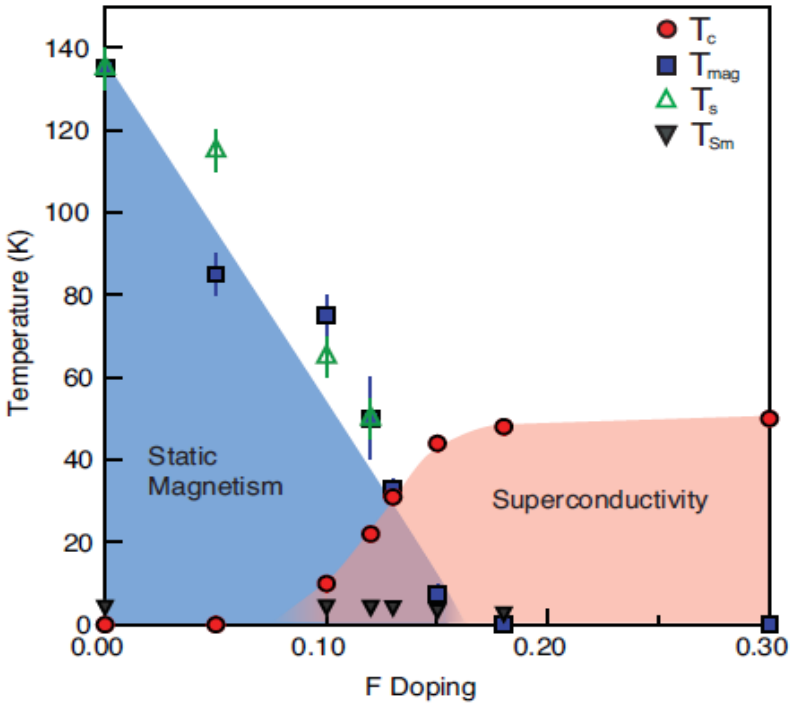

Fig. 1.4. Phase diagram of the magnetic and superconducting properties of $SmO_{1-x}F_xFeAs$. There is a clear region of coexistence between x=0.10 and x=0.15. T_c reaches its maximum value when the main static magnetism phase disappears. Evolution of the main magnetic transition temperature T_{mag}, the Sm ordering temperature T_{Sm}, the superconducting transition temperature T_c and the structural transition T_s, as a function of the F-doping concentration [38].

In 2006, Kamihara et al. [39] synthesized LaOFeP compound using the solid state reaction method and they reported a new class of superconductor with superconducting transition temperatures of T_{onset}=5 K and $T_{\rho\approx0}$=3.2 K. In 2008, Y. Kamihara et al. [31] prepared an iron-based La-oxypnictide quaternary phase LaOFeAs. Through electron F-doping, $LaO_{1-x}F_xFeAs$ showed superconducting transition T_c=26 K at F-doping content of x=0.11 (11% oxygen is replaced with fluorine) when oxygen was partially replaced by fluorine in this phase. Through electron or hole doping, iron-based oxypnictides LnOFeAs showed a superconducting transition, evident in the drop at a certain temperature, in the curves of resistivity and in magnetic susceptibility [5,8,31,40,41,42]. The maximum transition temperatures were observed in Sm-oxypnictide $SmO_{0.8}F_{0.2}FeAs$ with T_{onset}=56.1 K and $T_{\rho\approx0}$=54.1 K [43]. In addition, Gd-oxypnictide $Gd_{0.8}Th_{0.2}OFeAs$ showed an onset transition temperature near 56 K [44].

Iron-oxypnictide superconductors include the LnO and FePn layers, which are stacked alternately along the c-axis. The parent compounds for these superconductors consist of $(FePn)^{\delta-}$ layer, which forms a square iron lattice sandwiched by $(LnO)^{\delta+}$ layers. In the parent iron-pnictide LaOFeAs, the $(La^{3+}O^{2-})^{1+}$ layers act as a charge reservoir, while the $(Fe^{2+}As^{3-})^{1-}$ layers are conduction layers. The superconductivity is activated with the increased carrier density in one or both layers. For example, the substitution of O^{2-} with F^{1-} in the LaO layers, $LaO_{1-x}F_xFeAs$ [31], supply an extra positive charge into the insulating layer and a negative charge into the conduction layer of the parent compound. The replacement of Nd^{3+} with Th^{4+} in the NdO layer ($Nd_{1-x}Th_xOFeAs$) [45], $La^{3+}$with Sr^{2+} ($La_{1-x}Sr_xOFeAs$) [46], La^{3+} with Ce^{3+} ($La_{1-x}Ce_xO_{0.9}F_{0.1}FeAs$) [5], and As^{3-} with Sb ($LaO_{0.8}F_{0.2}FeAs_{1-x}Sb_x$) [42] cause the occurrence of superconductivity in the first two compounds and

enhancement of the superconducting transition temperature in other two compounds. Thus, ion substitution doping provides more or less holes or electrons into the system depending on hetero- or homovalent.

1.2 Problem statements

The phenomenon of superconductivity is predicated in the normal to superconducting phase transition. Superconducting phase transition at the critical transition temperature (T_c) is administered by lattice vibrations as electron pairs (Cooper pairs) mediated by phonons. Cooper pairs can appear above T_c, thus requiring the presence of a coexisting state of normal and superconducting phases under two possibilities. This state is related to the basic system at room temperature or it begins to occur at the T_{pair} of the forming electron pair, where $T_{pair} > T_c$.

Although the phonon variation reflects the Cooper-pair state at $T>T_c$ and $T<T_c$, but the parameters (e.g., superconducting energy gap and transition temperature) that describe the superconductor are related to the electronic state at $T\leq T_c$.

The picture is incomplete, given that the role of the superconductivity cannot be reduced for $T<T_c$ only. Thus, determining the features of the phonon behavior of the superconductive property is important. Thus, this study aims to identify the energy gap that can characterize or is related to the phonon state of specific heat at $T>T_c$.

1.3 Research objectives

The principal objectives of this project can be summarized in the following points:

1. To study and model the normal-superconducting phase transition of the superconducting specific heat *C(T)* of iron-oxypnictide superconductors.

2. To synthesize a new iron-based superconductor branching from the oxypnictides family by replacing Pnictogen (Pn) with Germanium (Ge) (i.e. $LaO_{1-x}F_xFeGe$ compounds).
3. To study the temperature dependence of electrical resistivity *ρ(T)*, and probe the energy gap Δ in the FTIR spectra of these compounds.
4. To demonstrate the transition feature of *C(T)* by applying the proposed model on the synthesized compound, and on the iron-oxypnictide superconductors.

1.4 Scope of the research

In this research of the superconducting properties of iron-based $LnO_{1-x}F_xFeAs$ (Ln= La, Sm) oxypnictide and $LaO_{1-x}F_xFeGe$ phases, attention was concentrated on two aspects in order to obtain the superconducting parameter at room temperature which related to pairing mechanism:

First, the modeling of temperature dependence of specific heat of $LnO_{1-x}F_xFeAs$ (Ln= La, Sm) compounds by the coexistence of normal and superconducting state.

Second, the study of infrared spectroscopy of $SmO_{1-x}F_xFeAs$ and $LaO_{1-x}F_xFeGe$ at room temperature through phonon effects in normal state specific heat, where the transition in phonon suppression features from a non-superconducting to a superconducting sample can be observed.

1.5 Originality of the research

The originality of this research appears in following two points:

First, a model of superconductivity transition based on the superconductive behavior of specific heat was introduced. In this model the gap opening in the phonon specific heat when the system enters the superconducting state was assumed, which means that the energy gap related to phonon state rather than electronic state.

Second, all previous studies on LnOFePn compounds used Pnictogen (Pn), Arsenic (As), or Phosphorus (P). Given the importance of the FePn layer in superconductivity, the replacement of Pn with another element opens the way for a new compound and possibly shows specific properties, reflecting the effectiveness of this element in the conduction layer. We chose Germanium (Ge) to fill the place of Pn in the F-doped LaOFeGe, for the following reasons:

1. Ge exhibits superconductivity at about 0.5 K in gallium-doped germanium (Ga-doped Ge) at ambient pressure [47], where the annealing at 850 °C can create a superconducting condensate in a Ga-doped Ge [48].
2. The Ge in a binary compound Nb_3Ge (T_c=23.2 K [33]) has a significant impact in promoting superconductivity; T_c=9.2 K for Nb [33].
3. The magnetic state of the FeGe compound [49,50,51,52], similar to FeAs [53,54,55] compound, showed a phase transition from paramagnetic to helimagnetic order at phase transition temperature. The temperature point of the phase transition of binary FeAs compound was observed in the temperature dependence of resistivity *ρ(T)* [54] and specific heat *C(T)* [55].
4. Moreover, Ge costs less and is safer than the toxic As.

1.6 Outline of the thesis

The outline of the thesis is as follows: Chapter 2 deals with a literature overview of the main properties of iron-oxypnictide superconductors and methods of synthesis in this family. Chapter 3 presents the crystal structure, as well as the theoretical models that investigate the superconductivity mechanism in iron-based oxypnictides. The methodology and instrumentation used in this thesis are described in Chapter 4.

Chapter 5 presents the theoretical and experimental results and discussion. The details on the transition temperature model, constructed based on the superconductive behavior of FeAs-based oxypnictides, as well as the obtained experimental results of the synthesized compounds $LaO_{1-x}F_xFeGe$ (x=0.0, 0.11, 0.13) are presented in this chapter. Finally, Chapter 6 presents the conclusions of our entire research and the suggestions for future work.

CHAPTER 2

LITERATURE REVIEW OF SUPERCONDUCTING Fe-BASED 1111 OXYPNICTIDES

2.1 Introduction

This chapter presents a literature review on iron-oxypnictide materials, beginning with the physical properties. Superconducting transition temperature which is associated with temperature dependence of resistivity and specific heat capacity, and superconducting energy gap which is related with FTIR spectra, are addressed. Finally the methods of synthesis are presented.

2.2 Physical properties

2.2.1 Temperature dependence of specific heat capacity

The heat capacity measurements proved the existence of phase transition because of the presence of a sudden jump or discontinuity, which was associated with the transition point of electrical resistivity and magnetic susceptibility of the superconductor [56,57]. This jump provided a realistic picture of transition from normal to superconducting state of some classes. These measurements enabled the reference of density of states [58] and prediction of the gap-node of the superconducting state [59].

For the 122-phase AT_2Pn_2 (A=Ba, Sr, Ca, or Eu; T=Fe or Ni; and Pnictide Pn=P or As) superconductors family, the transition from normal to superconducting state was clearly visible in the heat capacity curves. In compounds $BaNi_2As_2$ (Figure 2.1) [60], $Ba_{0.6}K_{0.4}Fe_2As_2$ [61], $Sr_{0.6}K_{0.4}Fe_2As_2$ [62], and $BaFe_{1.90}Pt_{0.10}As_2$ [63], the *C/T (J/mol.K^2) vs. T(K)* curve exhibited a jump in the first two samples. The curve also showed a discontinuity in another two samples at the superconducting transition temperature of resistivity and magnetic susceptibility, which were 0.7 K, 36.5 K,

35.6 K, and 23 K for $BaNi_2As_2$, $Ba_{0.6}K_{0.4}Fe_2As_2$, $Sr_{0.6}K_{0.4}Fe_2As_2$, and $BaFe_{1.90}Pt_{0.10}As_2$, respectively.

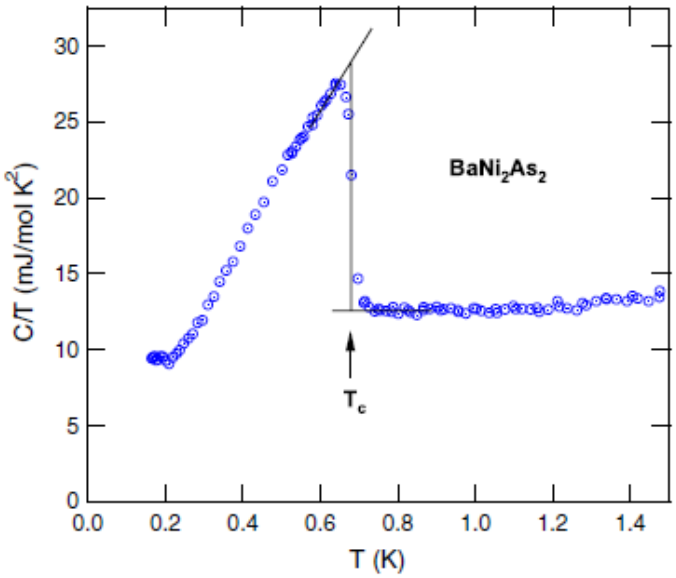

Fig. 2.1. Temperature dependence of specific heat capacity of $BaNi_2As_2$ compound. A jump at T_c was observed this curve [60].

In the 1111-phase *LnOMPn* (*Ln*-rare-earth, *M*-transition metals, *Pn*-P or As) superconducting family, the heat capacity jump was not visible as an anomaly point in the typical curves *C/T* vs. T^2 [59] and *C/T* vs. *T* [64] for $LaO_{0.9}F_{0.1}FeAs$ as shown in Figure 2.2. This disappearance, which is attributable to the small superfluid density or condensation energy [59], did not exist in $LaO_{0.9}F_{0.1}NiAs$ (T_c=3.8 K) but turned to a sharp jump at a critical temperature because of strong electron-phonon coupling [56].

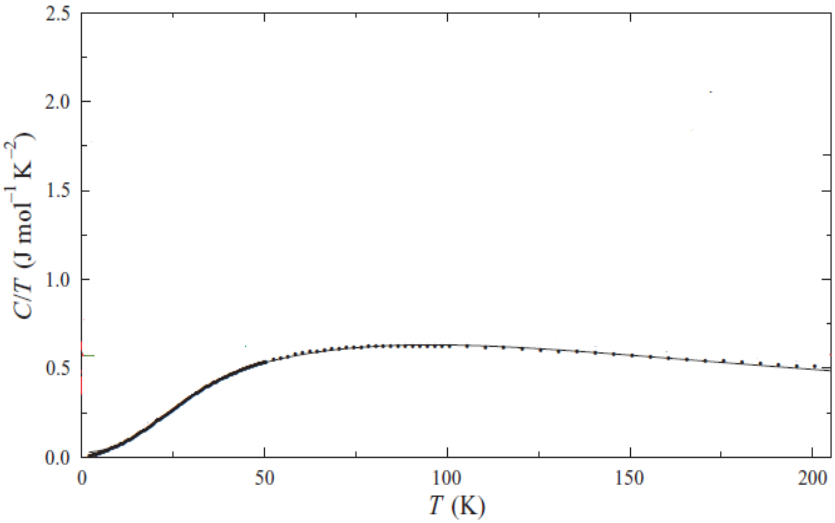

Fig. 2.2. Temperature dependence of specific heat capacity for $LaO_{0.9}F_{0.1}FeAs$ compound [64]. The jump was not visible in this curve.

At lower than T_c, the electron-phonon coupling descended as a result of the small contribution of one of them in heat capacity, which required the emergence of a jump [65]. Clearly, there was an obvious dependence of specific heat on the density of states by applying a multiple superconducting gap model. However, the T_c jump at the single gap was more pronounced than at the multiple gaps [66]. In the sample $LaOFe_{0.89}Co_{0.11}As$ below $T_{c,onset}$=14.3 K [40], little change was noted in the *C/T* vs. T^2 curve. This is no a jump but a deviation from data extrapolation. Further, it is not correct to assume that this is a broad specific-heat anomaly because the interpretation carries the meaning of jump.

For the undoped SmOFeAs, the specific heat jump was at 130 K and the anomaly was near T_c (50 K) for F-doping x=0.20 [67]. $SmO_{1-x}F_xFeAs$ has a higher transition temperature, depending on the high superfluid density, which is associated with the behavior of heat capacity. However, that is not so for $LaO_{1-x}F_xNiAs$, which has a low transition temperature and sharp jump. Another aspect of heat capacity is the absence of a jump in the *C* vs. *T* curve, although it appeared in the difference in the electronic contribution $C_e(x)$-$C_e(x=0)$ vs. *T* of the superconducting $LaO_{1-x}F_xFeAs$

and non-superconducting (LaFeAsO; $x=0$) samples [68]. Although there is a jump in the C/T vs. T^2 curve of the $LaO_{0.9}F_{0.1}NiAs$ sample, accurate parameters (such as the electronic and lattice heat capacity coefficient at normal state) were obtained by separating electronic and phonon normal state specific heat contributions from the superconducting system. Thus, the fitting was applied in the difference in specific heat at 10 T and at zero-magnetic field $(C_{0T}-C_{10T})/T$ vs. T/T_c [56].

Total specific heat in metal is $C=\gamma T+\beta_1 T^3$ [69] at a temperature much less than the Fermi temperature by considering the electrons, and the Debye temperature by considering the phonons. In the *LnOMPn* superconducting family, the C/T vs. T^2 curves below 8 K for $LaO_{1-x}F_xFeAs$ (x=0.05, 0.11, and 0.14) have the behavior of temperature dependence $C=\gamma_{sc}T+\beta_1 T^3$, where γ_{sc} is the electronic heat capacity coefficient affected by the spin fluctuation below 6 K for x=0 and 0.025 [68]. In the $LaO_{0.9}F_{0.1}NiAs$ system, the above temperature dependence formula is applicable above T_c, with the replacement γ_{sc} to γ_n. Based on this dependence, the entropy difference was not conserved above T_c [56]. In addition, the previous temperature dependence was fitted to $C(T)$ data for SmOFeAs and $SmO_{1-x}F_xFeAs$ (x=0.07, 0.15) between 15 K and 25 K [70].

2.2.2 Temperature dependence of resistivity

Iron-based LnOFeAs phase is not a superconductor and displayed an anomalous change in the slope of $\rho(T)$ resistivity measurement curve. The anomaly transition point related to the spin-density wave fluctuations and structural phase transition was at 150 [31], 145 (Figure 2.3) [17], 155 [71], 140 [72], 135 [44], and 124 K [41] for compounds LaOFeAs, CeOFeAs, PrOFeAs, SmOFeAs, GdOFeAs, and TbOFeAs, respectively. Conversely, nickel-based quaternary oxypnictides LaONiP and LaONiAs exhibited superconducting transition in resistivity

measurements with critical transition temperature T_{onset}=4 K ($T_{\rho\approx0}$=2 K) [73,74] and T_{onset}=2.4 K ($T_{\rho\approx0}$=2 K) [75], respectively. Moreover, in iron-based 1111-phase, only the LaOFeP compound [6,76] was a superconductor at T_{onset}=5 K ($T_{\rho\approx0}$=3.2 K) [39]. Table A1.1 (Appendix 1) presents the superconducting transition temperature of electrical resistivity *ρ(T)* measurements of the quaternary family LnOMPn oxypnictides.

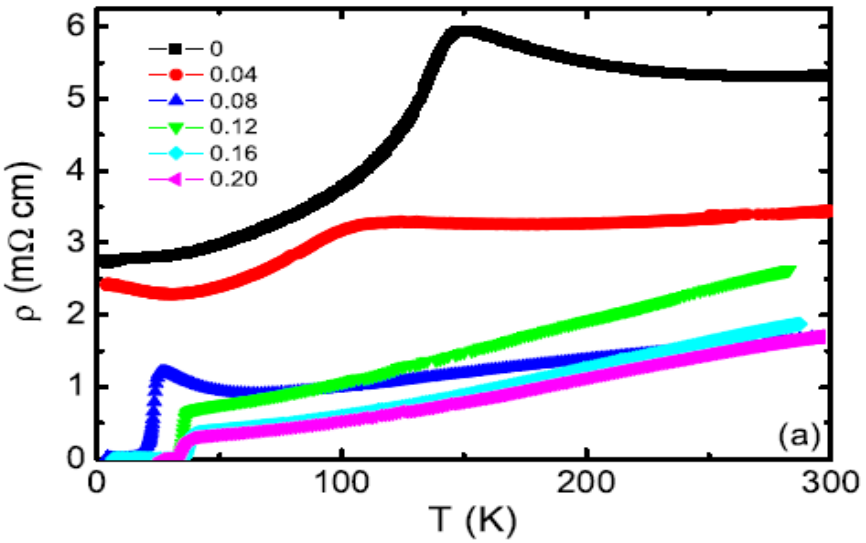

Fig. 2.3. Temperature dependence of electrical resistivity for $CeO_{1-x}F_xFeAs$, where the resistivity anomaly around 145 K at x=0 [17].

2.2.2.1 Doping effect

Superconductivity could be obtained from LnOFeAs phase through replacement of O^{2-} with F^- (i.e., F-doping), with the resulting phase being the $LnO_{1-x}F_xFeAs$ compound. Superconducting transition temperature T_{onset} of $LaO_{1-x}F_xFeAs$ was at 17 [16], 28 [16], 24.6 [77], and 30 K [31] for x=0.03, 0.06, 0.10, and 0.11, respectively. Figure 2.4 shows the F-doping dependence of T_c and T_{onset} on $LaO_{1-x}F_xFeAs$ [31]. After superconductivity appears, T_c is nearly unchanged up to x=0.14, and the highest T_c=26 K (T_{onset}= 30 K) is attained at the F-content x=0.11. Replacement La in $LaO_{1-x}F_xFeAs$ compound with other rare earth elements (Ce, Pr, Nd, Sm, Eu, Gd, Tb, Dy, and Tm) led to superconductors with T_{onset} > 28 K.

T_{onset}=42.5 [78], 52 [79], 52 [80], 56.1 [43], 36.6 [81], 45.9 [82], and 45.4 K [82] for compounds $CeO_{0.8}F_{0.2}FeAs$, $PrO_{0.89}F_{0.11}FeAs$, $NdO_{0.82}F_{0.18}FeAs$, $SmO_{0.8}F_{0.2}FeAs$, $GdO_{0.83}F_{0.17}FeAs$, $TbO_{0.8}F_{0.2}FeAs$, and $DyO_{0.9}F_{0.1}FeAs$, respectively. Two rare earth elements, Eu and Tm, did not display superconducting transition in resistivity measurements of $LnO_{0.84}F_{0.16}FeAs$ phase; instead, resistivity ρ(T) displayed metallic behavior [83].

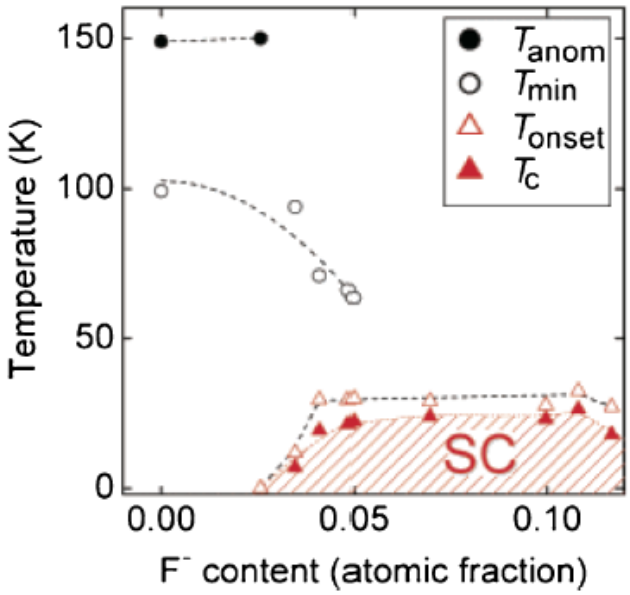

Fig. 2.4. Schematic diagram of F-doping dependence of T_c and T_{onset} on $LaO_{1-x}F_xFeAs$ compound [31].

Superconductivity in LnOFeAs phase can also be obtained by partially replacing the trivalent ion Ln^{3+} with a bivalent dopant, such as Sr^{2+}, Pb^{2+}, or a tetravalent dopant, such as Th^{4+} in the LnO layer. As a result, superconducting transition T_{onset} of superconductors Sr-doped $La_{0.87}Sr_{0.13}OFeAs$ [46] and Pb-doped $La_{8.0}Pb_{0.2}OFeAs$ [5] was at 25.6 ($T_{\rho\approx0}$=15 K) and 11.6 K ($T_{\rho\approx0}$=9.7 K), respectively. In Th-doping, which provides the insulating layer with an extra positive charge, superconductors $Nd_{0.8}Th_{0.2}OFeAs$ [45], $Gd_{0.8}Th_{0.2}OFeAs$ [44], $Tb_{0.9}Th_{0.1}OFeAs$ [41], and $Tb_{0.8}Th_{0.2}OFeAs$ [41] were successfully synthesized, exhibiting transition

temperature T_{onset} in resistivity measurements at 47, 56, 45, and 52 K, respectively, all higher than the recorded values for Sr- and Pb-doped compounds.

The third method of doping in the LnO layer consists of replacing the trivalent ion Ln^{3+} and monovalent ion F^- with two dopants, and is referred to as double doping. For K doping in $LaO_{1-x}F_xFeAs$ compound, the onset of superconducting transition was practically unaffected by the addition of K, with onset T_{onset} occurring at 26.20 and 26.45 K for $(La_{0.85}K_{0.15})(O_{0.85}F_{0.15})FeAs$ and $(La_{0.8}K_{0.2})(O_{0.8}F_{0.2})FeAs$, respectively [84]. Replacing potassium (K^{1+}) with Ce or Yb increased transition temperature T_{onset} to 29 K for $La_{0.2}Ce_{0.8}O_{0.9}F_{0.1}FeAs$ [5] and 31.3 K for $La_{0.9}Yb_{0.1}O_{0\cdot8}F_{0\cdot2}FeAs$ [85].

Superconductivity can be also achieved by doping in the conduction layer MPn (M=transition metals, and Pn=pnictogen). For Co-doped $LaOFe_{1-x}Co_xAs$ samples, the T_{onset} was at 11.2, 14.3, and 6 K for x=0.05, 0.11, and 0.15, respectively [40]. Co-doping for $PrOFe_{1-x}Co_xAs$ samples showed T_{onset} at 4.7, 14.2, and 5.9 K for x=0.05, 0.1, and 0.15, respectively [71]. For $SmOFe_{1-x}Co_xAs$ samples, T_{onset} (=15.2 K) was unchanged at two levels of doping x=0.10 and 0.15 [86], whereas T_{onset} was affected by the change in doping from x=0.10 to x=0.15 for Co-doping in La-oxypnictide and Pr-oxypnictide samples. Ir-doped $SmOFe_{0.85}Ir_{0.15}As$ compounds provided the critical transition temperature T_{onset} close to 17.3 K [8], which is greater than that for Co-doping. In [42], researcher reported one case of increased transition temperature T_{onset} with doping in the conducting layer when $LaO_{0.8}F_{0.2}FeAs$ was synthesized with Sb-doping. The doping in this case was in both layers and led to the enhancement of transition temperature to 30.1 K for compound $LaO_{0.8}F_{0.2}FeAs_{0.95}Sb_{0.05}$.

The critical superconducting transition temperature for 1111-oxyarsenide compounds is affected by a number of factors, mainly the density of conduction carriers in the insulating and conduction layers, which is altered with doping as mentioned above. Although hole or electron-doping suppressed the anomalous behavior to induce superconductivity, some phases did not show superconductivity: $La_{0.80}Sr_{0.20}OFeAs$ (T_{onset}=25.6 K for x=0.13) [46], $LaOFe_{0.80}Co_{0.20}As$ (T_{onset}=14.3 K for x=0.11) [40], $PrOFe_{0.70}Co_{0.30}As$ (T_{onset}=14.2 K for x=0.10) [71], $EuO_{0.84}F_{0.16}FeAs$, and $TmO_{0.84}F_{0.16}FeAs$ [83]. For nonsuperconducting $La_{0.80}Ce_{0.20}OFeAs$ compound [5], the doping was at the same oxidation state (La^{3+} was replaced with Ce^{3+}), and as a result, anomaly point T_{anom} still existed and appeared at 155 K. In general, no direct evidence or rule has been discussed to predict the transition behavior in resistivity after doping. However, certain factors cause changes in the interactions among electrons (i.e., electron scattering and electron-phonon scattering).

2.2.2.2 Effect of external pressure

Another factor that significantly affects transition temperature in 1111-oxypnictides is external pressure P. First, the temperature dependence of electrical resistivity for compounds was synthesized under high pressure. Resistivity measurement of $LaO_{0.4}F_{0.6}FeAs$ compound (which was prepared under high-pressure synthesis conditions at 6 GPa for 2 h at 1250 °C) showed that transition temperatures T_{onset}=41 K and $T_{\rho\approx0}$=30 K were higher than that prepared by ambient pressure synthesis (AP) [87]. The highest T_c of La-oxypnictides obtained under high-pressure synthesis (HP) can be attributed to the large shrinkage of crystal lattice on the Fe-As plane because of sufficient F-doping observed in high pressure $LaO_{0.4}F_{0.6}FeAs$ compound compared with ambient pressure LaOFeAs compound [87]. For Pr-

oxypnictides, the highest T_{onset} was obtained for samples prepared using HP method [79], whereas in Sm-oxypnictides, the highest T_{onset} was obtained for samples prepared by AP synthesis method [43]. However, $SmO_{0.85}F_{0.15}FeAs$ prepared using HP method has higher superconducting transition temperature compared with the same sample prepared using the AP method [88]. Second, pressure affects the temperature dependence of electrical resistivity for compounds synthesized under ambient pressure. The onset transition temperature T_{onset} for $LaO_{0.89}F_{0.11}FeAs$ compound increased rapidly with pressure and increased dramatically from 26.3 K at ambient pressure to 43 K at static pressure P=4 GPa, whereas zero resistivity transition temperature $T_{\rho\approx0}$ increased at a slower pace. The broadening of the superconducting transition with the increase in pressure may be caused by strains on individual grains, inter-plane and intra-plane interactions, or/and lattice defects especially in insulating layers [89,90].

The external hydrostatic pressure dependence of superconducting transition temperature for compound $SmO_{1-x}F_xFeAs$ ($0.10 \leq x \leq 0.20$) appeared to be pressure-dependent (Figure 2.5), with T_c increasing with the increase in P for x=0.10 and x=0.12, whereas for $x > 0.12$ (x=0.15, 0.18, and 0.20), the compound displayed low sensitive dependence of T_c on P with inverse dependence (Figure 2.5), that is, T_c decreased with the increase in P (P=0.01 GPa to 1.2 GPa) [91]. The relation between T_c and pressure P depending on the doping level of the sample $SmO_{1-x}F_xFeAs$ was also reported by Lorenz et al. [92], where for x=0.30, transition point T_c decreased rapidly with pressure increase (P=0 GPa to 1.6 GPa). On the other hand, for x=0.13, T_c increased with pressure increase until 0.94 GPa and then remained stable at pressure range of 0.94 GPa to 1.5 GPa. Thus, for $SmO_{1-x}F_xFeAs$ compound, the change in pressure-induced superconducting transition T_c from enhancement to

suppression occurs between F-doping concentrations 0.13 and 0.15. The doping level effect and relation between T_c and pressure was determined through the comparative study of $LaO_{0.89}F_{0.11}FeAs$ and $CeO_{0.88}F_{0.12}FeAs$ compounds as reported by Zocco et al. [93]. An increase in superconducting transition with pressure for the first sample was observed, but when pressure was applied to the second sample, the superconducting transition decreased monotonically. This result is due to the optimum doping level that led to a maximum transition point of resistivity. The doping level of the first sample was under-optimum, whereas that of the second sample was close to optimum. However, an increase in pressure corresponded to an increase in carrier concentration in the FeAs layer, but the effect of pressure on T_c was more complicated than this simple interpretation (i.e., changing the carrier concentration) [93].

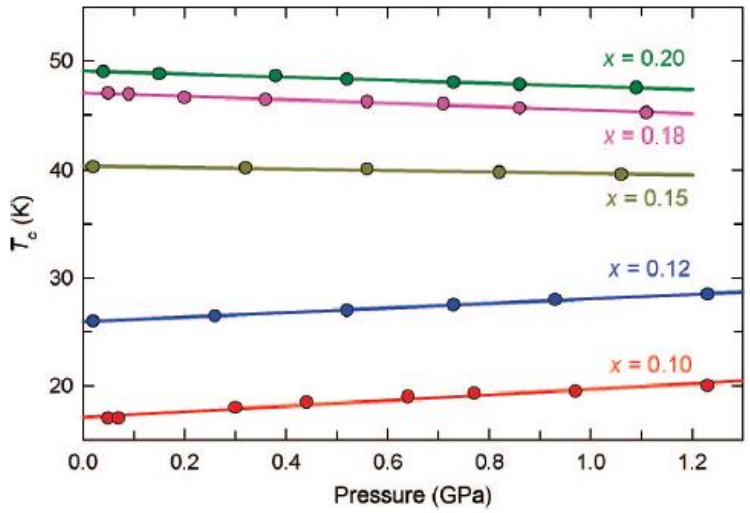

Fig. 2.5. Dependence of the critical temperature of $SmO_{1-x}F_xFeAs$ ($0.10 \leq x \leq 0.20$) on the external pressure P. T_c increases monotonically as the F-doping level x increases to 0.20 [91].

2.2.2.3 Effect of concentration and lattice parameters

Concentration and lattice parameters are also factors that affect superconducting transition temperature. Doping dependence of T_c, *a,* and *c* for hole-doped $La_{1-x}Sr_xOFeAs$ sample showed that *a* and *c* increased monotonously with Sr-doping concentration and a consequent increase in T_c. This expansion in lattice constants is because the radius of Sr^{2+} is larger than that of La^{3+} [94]. In contrast with electron doping, T_c increased with the shrinkage of lattice parameters, whereby the electron-doped $SmO_{1-x}F_xFeAs$ sample showed that *a* and *c* decreased monotonously with the increase in F-doping concentration x in the range of $0 \leq x \leq 0.20$, and T_c increased with the increase in concentration x in the same range [88].

When hole doping was applied in the FeAs layer for $PrOFe_{1-x}Co_xAs$ sample, the lattice parameters decreased with the increase in Co concentration x ($0 < x < 0.3$), but T_c increased from 4.7 K for x=0.05 to 14.2 K for x=0.1. However, transition temperature T_c decreased with higher Co-doping concentration $x > 0.1$ (T_c=5.9 K for x=0.15, T_c=4 K for x=0.20 and 0.30) [71]. A similar behavior of doping dependence of T_c, *a*, and *c* in double-doped compound $La_{1-x}Ce_xO_{0.9}F_{0.1}FeAs$ (x=0, 0.2, 0.4, 0.6, and 0.8) was observed. Lattice parameters *a* and *c* slightly decreased with the change in Ce concentration (*a*=4.029˚A and *c*= 8.726˚A at x=0, and *a*=3.994˚A, *c*=8.598˚A at x=0.8) whereas T_c increased from 24.99 K at x=0 to 29 K at x=0.8 with the presence of an abnormal point in the phase diagram $T_c(x)$ at x=0.60 (T_c= 28.01 K) as shown in Figure 2.6 [5]. In contrast to the case of $La_{1-x}Ce_xO_{0.9}F_{0.1}FeAs$, the transition temperature for $LaO_{0.8}F_{0.2}FeAs_{1-x}Sb_x$ compound (double-doping in both layers) decreased from 30.1 K at Sb concentration x=0.05 to 28.6 K at Sb concentration x=0.10. However, by increasing the doping level from x=0.05 to x=0.10, lattice

parameters *a* and *b* increased because of the larger size of the Sb ion compared with the As ion [42].

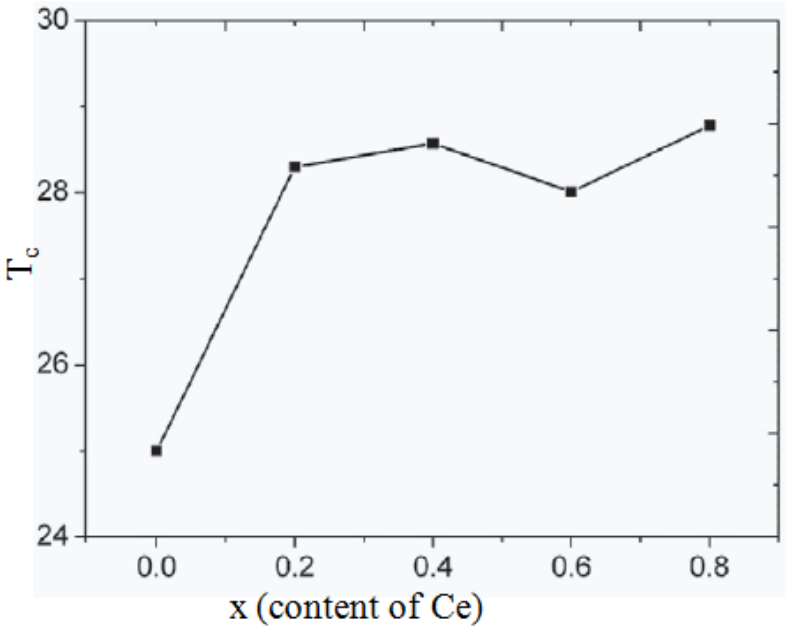

Fig. 2.6. Phase diagram showing the superconducting transition temperatures as a function of the Ce doping level in $La_{1-x}Ce_xO_{0.9}F_{0.1}FeAs$ compound [5].

2.2.2.4 Sintering temperature effect

The effect of sintering temperature on the superconducting properties of $SmO_{0.8}F_{0.2}FeAs$ was reported by Wang et al. [43] as shown in Figure 2.7. Onset transition temperature of the samples sintered at 850 ºC was 53.5 K. Samples sintered at 1000 ºC displayed a transition temperature of 56.1 K whereas those sintered at 1200 ºC displayed a transition temperature of 50.8 K. Samples sintered at 1000 ºC had the highest transition temperature, the lowest $\rho(T)$, and the highest residual resistivity ratio ρ(300 K)/ρ(57 K), indicating low impurity scattering and enhanced carrier density [43]. However, the highest onset transition temperature was related to specific sintering temperature, where T_{onset} was 41 K for $SmO_{0.7}F_{0.3}FeAs$ sample sintered by a two-step approach at 500 ºC for 15 h and then at 900 ºC for 40 h [95], and it was 54.6 K for sintering at 1160 ºC for 40 h [96].

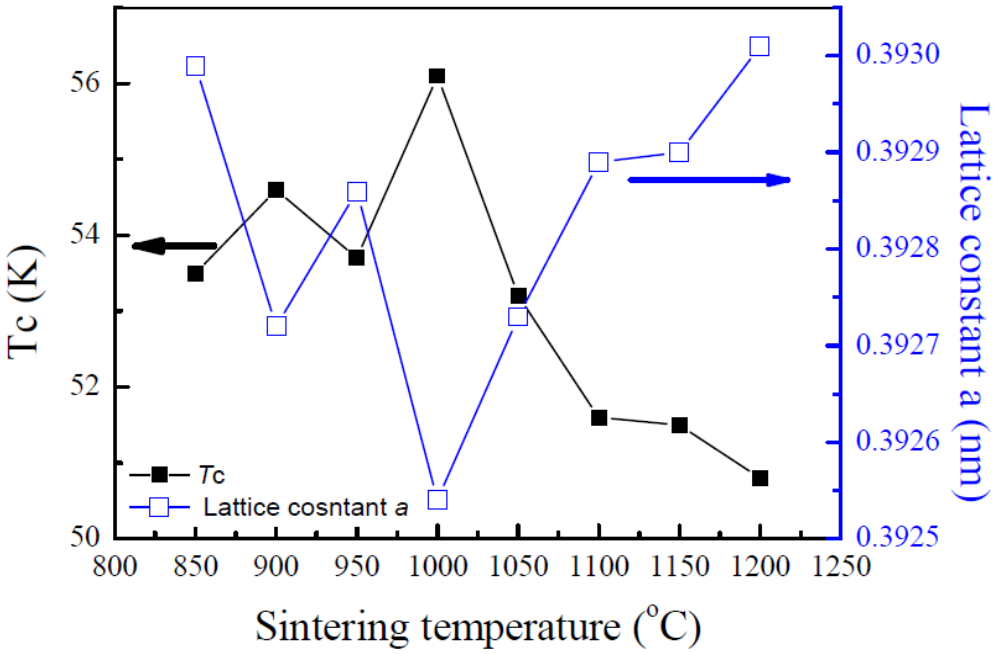

Fig. 2.7. Dependence of the lattice constant and onset transition temperature on the sintering temperature for $SmO_{0.8}F_{0.2}FeAs$ samples [43].

2.2.2.5 Effect of magnetic field

One of the important factors affecting superconductivity is magnetic field. Temperature dependence of resistivity under different magnetic fields for $LaO_{0.9}F_{0.1}FeAs$ [15,97], $La_{1-x}Yb_xO_{0.8}F_{0.2}FeAs$ [85], and $NdO_{1-x}F_xFeAs$ (x=0.12,0.18) [80,98] compounds showed that onset transition T_{onset} shifts to a lower temperature with an increase in magnetic field, but zero resistance transition $T_{\rho\approx0}$ shifts more quickly. However, the transition width gradually broadens with an increase in the magnetic field. The effects of magnetic field in superconductors can be attributed to the weak-link behavior of grain boundaries. Onset transition temperature occurs when the grains become superconducting and is restricted by the upper critical field of these individual grains, whereas zero-resistance transition is determined by the presence of superconducting transition among and within grains. Weak coupling strength among grains, called weak-link, is responsible for the magnetic field dependence of the resistivity transition curve. The magnetic field can break this link